



Numerical study on tunnel damage subject to blast loads in jointed rock masses

Shujie Chen¹ · Zhengguo Zhu^{1,2}

Received: 24 August 2021 / Accepted: 29 November 2022 / Published online: 10 December 2022
© The Author(s), under exclusive licence to Springer-Verlag GmbH Germany, part of Springer Nature 2022

Abstract

Drill and blast method is an accepted technique of tunnel excavation but it often causes over-break or even threatens the stability of the surrounding rock. Moreover, the rock mass mostly contains different forms of discontinuities and so more severe damage may develop under the blasting loads. In this paper, numerical modeling on the damage of jointed tunnel excavation subject to blast shock was carried out with three-dimension Distinct Element Code (3DEC). The blast-induced damage zones (BIDZ) including failure zones and open zones are as evaluation indicators. The effects of joint geometrical and mechanical properties, tunnel depth and advance length on damage depth were evaluated. The influence extent of these factors was also compared by arithmetic mean of maximum damage depth and its standard deviation. Lastly, the results are contrasted with an existing empirical formula. It is found that increasing advance length has a more obvious effect on tunnel damage comparing with other factors, and failure zones begin to develop when the advance length exceeds 2 m in the model. If the joint inclination angle increases above 60°, the tunnel is prone to instability and the failure rocks is mainly found at the tunnel roof. For all joint strike angles, there is a clear damage zones in the surrounding rock, and failure zones are mainly located at the sidewall. The damage depth is highly dispersive within 1 m of the joint spacing. This research provides an insightful understanding of damage magnitude of jointed rock mass during tunnel excavation with blasting.

Keywords Drill and blast method · Three dimension Distinct Element Code (3DEC) · Blast-induced damage zones (BIDZ) · Joint properties · Advanced length

Introduction

Drill and blast method (D and B) is a cost-effective and flexible way in the excavation of underground structures including mining, quarrying and tunneling. But the approach has an unavoidable drawback because it leads to a blast-induced damage zone (BIDZ) in the surrounding rock due to explosive shock. Besides, there are frequently different types of discontinuities including foliation, faults and joints in natural rock mass (Azarafza et al. 2017). When the shock wave

encounter these discontinuities, it will be reflected and generate tensile stress wave, thus cause more extended cracks in the surrounding rock (Trisugiwo et al. 2016). A series of problems will also be provoked:

potentially unstable rocks (Wang et al. 2020), increasing permeability (Zhang et al. 2021), secondary treatment costs, and severe rock mass damage can even cause the tunnel destabilization. Thus, it is of great importance to investigate the dynamic response for tunnels containing numerous discontinuities.

Many research efforts have been made to conduct studies on tunnel damage issues. For example, Holmberg (1979) developed the smooth blasting technique which can reduce the rock damage and form a flatter profile. Many field investigations and model predictions are also used to study the stability of jointed rock mass (Azarafza et al. 2018; Dey and Murthy 2012; Foderà et al. 2020; Han et al. 2016; Koopialipoor et al. 2019). These methods are helpful to improve the effectiveness and safety of tunnel excavation. But due to the difficulty of setting joints in laboratory experiment and the

✉ Shujie Chen
chenshujie5666@163.com

Zhengguo Zhu
zzg@stdu.edu.cn

¹ School of Civil Engineering, Shijiazhuang Tiedao University, Shijiazhuang 050043, China

² Key Laboratory of Roads and Railway Engineering Safety Control, Ministry of Education, Shijiazhuang Tiedao University, Shijiazhuang 050043, China

limitation of monitoring capability in field test, the research on jointed tunnel damage under internal blasting influence is not extensive.

Numerical methods have been widely applied for blasting damage analysis for its cost performance and convenience. The commonly implemented programs for jointed rock tunnel include Finite Element Method (FEM), Discrete Element Method (DEM) and hybrid Finite Discrete Element Method (FDEM), as shown in Table 1. The FEM programs including AUTODYN, LSDYNA and ABAQUS are able to carry out the study of blasting, impact and collision with high calculational efficiency due to its explicit solving functionality. But since these programs are continuous numerical forms, they are not suitable for simulating the large deformation or failures during blasting as well as difficult to model discontinuities. In comparison, the DEM or FDEM is more applicable for modeling of cracking and casting process because it allows a large-scale sliding of the elements. The branches of DEM mainly include Particle Flow Code (PFC), Discontinuous Deformation Analysis (DDA), Universal Distinct Element Code (UDEC) and 3DEC (three-dimensional version of UDEC). For instance, Li et al. (2014) studied the dynamic reaction caused by the release of in situ stress during tunnel excavation through PFC. Zhao et al. (2011) investigated the effects of time delay and rock properties on tunnel blast-induced crack propagation by DDA method. Varma et al. (2019) evaluated the influence of geometrical properties of joints on tunnel stability under seismic loading based on UDEC. Deng et al. (2014) focused on the damage zones and peak particle velocity (PPV) around tunnel surface and studied the stability of tunnel subject to ground blasting shock wave under varied geometric and mechanical properties of joints through UDEC. Monsalve et al. (2019) used terrestrial laser scanning technology to statistically characterize the tunnel discontinuities and defined a discrete fracture network in 3DEC. Moreover, some hybrid FDEM codes have also been developed in the simulation of jointed tunnel such as FLAC-PFC (Saiang 2010) and Y-HFDEM IDE (Zhao et al. 2011).

Nevertheless, in the numerical methods above, although the coupled FDEM programs were used to analyze the

influence of damage zones on tunnel, the operation of joints is very complex in these codes (Xiao and Quan 2002), and they usually need to consume more computing time (Cai et al. 2013). Besides, there also are some limitations in DEM codes. For PFC, the determination of the rock mechanics parameters and joints attitude are complicated. The treatment of natural discontinuities in DDA are set as rigid (Ning et al. 2012). UDEC is a two-dimensional simulation process, but D and B in tunnel usually has a certain advance length. Comparatively, 3DEC is a three-dimensional numerical code and has an acceptable computational efficiency, while also applied to analyze the propagation behavior of shock waves in jointed rock mass (Malmgren et al. 2006), but it has not been sufficiently explored to investigate tunnel blasting mechanism and formation of damage zones.

The research aims to develop a tunnel excavation model based on 3DEC to study the surrounding rock damage subjected to blasting shock in jointed rock mass. The blast load is considered as a stress time history applied on the tunnel contour boundary. The BIDZ is employed as the evaluation indicator. The effects of some parameters on the tunnel damage are investigated. For finding the most significant factor affecting tunnel damage, a sensitivity analysis of these parameters is also performed. In the discussion, the results of this study are compared with an existing empirical formula.

Methodology

Research route

The main procedure for the research content is shown in Fig. 1. First, the equivalent blast shock wave and loading boundary are introduced. Then the modeling process, material properties and damage evaluating indicator are described and so the tunnel excavation model with D and B is formed. Subsequently, parametric studies were conducted, which mainly involved the effects of joints, stress distribution and advance length because these parameters have a relatively important influence on the stability of tunnel structure. In

Table 1 Numerical methods commonly used for jointed rock tunnel

Methods	Codes	Disadvantage	Advantage
FEM	AUTODYN、LS-DYNA、ABAQUS	Not suited for mesh large deformation Difficult to model discontinuities	High computational efficiency
DEM	PFC	Difficult to control the joints attitude	Cracking and casting process
	DDA	Disregard the joint deformation	
	UDEC	Limitation of 2D plane	
	3DEC	Median computational efficiency	
FDEM	FLAC-PFC、Y-HFDEM IDE	Higher CPU time and memory consumption	

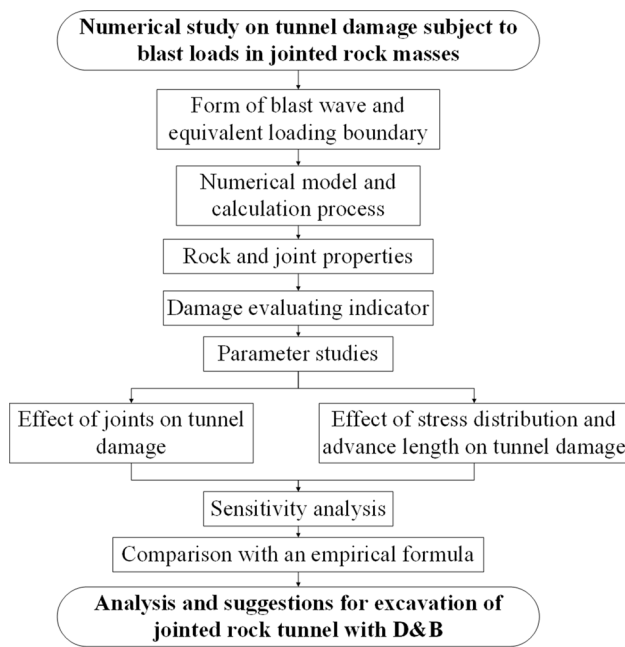


Fig. 1 Flow chart for the model generation and modeling process

the latter section, a sensitivity analysis of these parameters was performed, and the results of this model are also compared with an empirical formula and some suggestions are provided for jointed tunnels excavated with blasting.

The blast load on equivalent elastic boundary

As shown in Fig. 2, the rock between the contour holes and buffer holes is the burden layer. After detonation of the charges, the stress waves generated by the contour blastholes are reflected at the free surface and transform to tensile stress waves. Then the burden rock is shattered and a series of crater boundaries are formed. The tunnel profile is established by these crater boundaries, and the connecting line of the contour blastholes is referred as the equivalent elastic boundary.

Different from specialized dynamic analysis codes such as LSDYNA and AUTODYN, the parameters of explosive material cannot be added directly in 3DEC, thus the equivalent stress time-history of blasting load is widely adopted. The blast time-history is ideally obtained by monitoring the

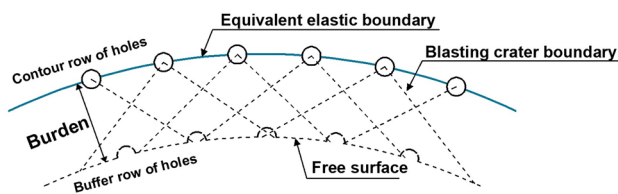


Fig. 2 Diagram of the equivalent elastic boundary

pressure around blastholes in the field experiment. But due to the extremely fast blasting process, it is difficult to monitor and extract the blasting load time-history from the explosion site. Hence, Lu et al. (2011) developed a semi-empirical formula for the blasting load versus time based on the Jones-Wilkinse-Lee (JWL) state equation. As shown in Fig. 3, the green dashed line is the equivalent blasting load. To use this time-history in 3DEC, it was simplified to the triangular load function $P_D(t)$ as shown in the solid red line, and its govern equations are given in Eqs. (1) and (2) (Yan et al. 2016).

$$P_D(t) = P_0 f(t) \tag{1}$$

$$f(t) = \begin{cases} \frac{t}{t_r} (0 \leq t \leq t_r) \\ \frac{t_z - t}{t_z - t_r} (t_r \leq t \leq t_z) \end{cases} \tag{2}$$

According to the Chapman-Jouguet model in a condensed explosive, for the uncoupled charge structure, the peak of initial explosion pressure P_0 on the blasthole wall is given by Eq. (3)

$$P_0 = \frac{\rho_0 D^2}{2(\gamma + 1)} \left(\frac{a}{b}\right)^{2\gamma} \tag{3}$$

where a is the charge diameter, b is the blasthole diameter, D is the detonation velocity, ρ_0 is the explosive density, γ is the ratio of the specific heats for the detonation gasses ($\gamma = 3$).

The blasting load applied to the equivalent elastic boundary meets the Saint-Venant’s principle (Lu et al. 2012), so it does not affect the dynamic response of far-filed rock mass. The mimetic blasting load $P_e(x, t)$ on the equivalent elastic boundary is shown in Eq. (4)

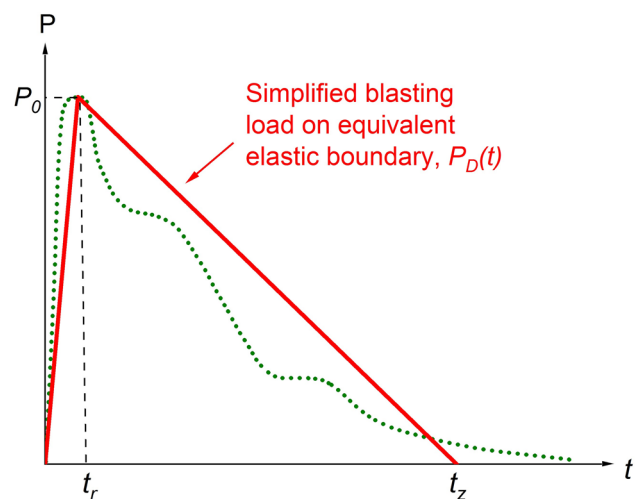


Fig. 3 Blasting load applied on the equivalent elastic boundary

$$P_e(x, t) = \frac{2r_0}{r_1} P_D(t) \tag{4}$$

where r_0 is the radius of the blasthole, r_1 is the distance between two contour blastholes.

The 2# emulsion explosive was adopted in this study and the detailed parameters are shown in Table 2. The initial explosion pressure P_0 can be calculated by substituting the data in Table 2 into Eq. 3. According to the consequence of Lu et al., the rising time of triangular load t_r and the total action time t_z should be adopted as 0.7 ms and 8 ms respectively for reasonably considering the movement of detonation gas (Lu et al. 2012).

Numerical model and calculation process

Bench blasting technique is a typical blasting method used in tunnel construction (Yu 2018). Some studies have shown that the over-breaking and rock damage of upper step is more severe under blasting load due to gravity and stress redistribution (Zhang et al. 2020). Accordingly, the numerical model in this study is designed as upper bench of semi-circular tunnel. The advance length variation is achieved by the change of model thickness. Figure 4 is the model diagram of the tunnel with an assumed width of 7 m, a height of 3.5 m. Considering the influence of boundary effect on dynamic analysis, the width and height of the entire model are both 75 m because it can minimize the interference of boundary on blasting process when the ratio of model size to tunnel diameter is more than 10. The setup of the joints is described in details in the section of parameter studies. The

modeling procedure is mainly divided into three stages, as shown in Fig. 4:

- (a) Initial stress was generated throughout the model, where fixed boundary condition was applied at the bottom, and zero velocity in X-direction was applied at lateral boundaries, while the top boundary was treated as stress boundary.
- (b) The blastholes inside the tunnel contour usually cause minor damage to the surrounding rock. Thus, after the completion of initial balance calculation, the rock mass inside the contour blastholes were removed to simulate the tunnel excavation.
- (c) The blasting load time-history was applied to the tunnel profile surface (also as equivalent elastic boundary), and at this stage all the boundaries of model were replaced with non-reflection boundaries.

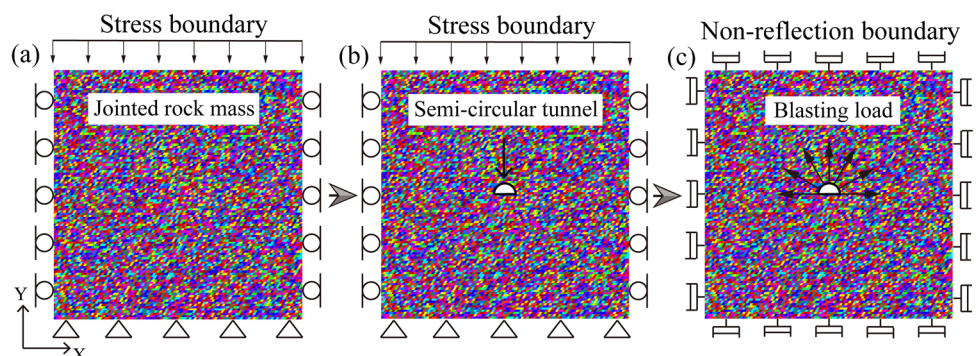
Rock and joint properties

The response of the rock masses under dynamic loading is different from that under static loading, so the mechanical parameters of rock should be set as the dynamic parameters. Besides, after the excavation of underground opening, a certain extent of damage will be incurred within the surrounding rock (Read 2004). Research from the underground laboratory also shown that for tunnels constructed by the drill and blast method, the rock in the vicinity of the tunnel profile is subject to both blast shock waves and in-situ stress redistribution, usually yielding more severe damage (Martino and Chandler 2004). In contrast, the rock relatively far from the contour is only affected by the ground stress redistribution. In the numerical model, the blasting process of the blastholes inside the tunnel contour is simplified by removing the interior rock mass. Therefore, prior to the application of blast shock wave, excavation damage zones (EDZ) have been formed in the surrounding rock around the equivalent elastic boundary. To consider the effect of internal rock excavation, we classify the rock around tunnel

Table 2 Explosive parameter

Blasthole diameter b (mm)	Charge diameter a (mm)	Explosive density ρ_0 (kg/m ³)	Detonation velocity D (m/s)
42	35	950	3700

Fig. 4 3DEC tunnel model in jointed rock masses subject to blasting load: **a** initial equilibrium **b** removing rock block in inner blastholes **c** application of blasting load



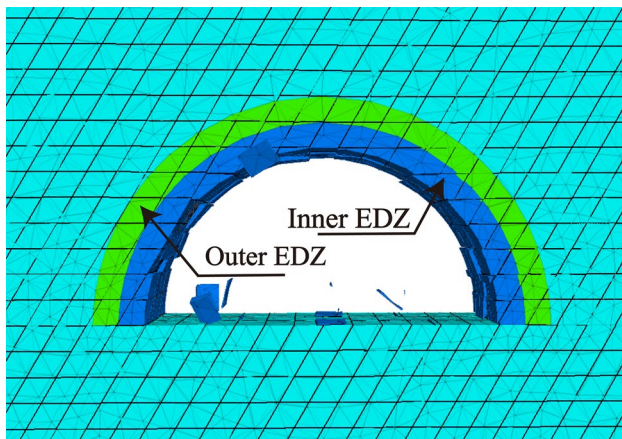


Fig. 5 Diagram of inner and outer EDZ

Table 3 Rock properties in different zones around the tunnel surface (Lu et al., 2011)

Special zones	Virgin rock	Tunnel wall perimeter	
		Inner EDZ	Outer EDZ
Dynamic elastic modulus (MPa)	47,200	37,800	42,500
Density(kg/m ³)	2700	2700	2700
Dynamic Poisson' ratio	0.23	0.27	0.25

excavation perimeter into two thin weak layers as inner EDZ and outer EDZ, respectively.

The depth of inner and outer weak layers is supposed to be respectively 0–1.0 m and 1.0–2.0 m adjacent to the tunnel contour, as shown in Fig. 5. The detailed rock mass parameters are shown in Table 3, corresponding to granite rock mass, and are obtained through laboratory and numerical tests (Lu et al. 2011).

For the joint stiffness value, many studies have shown that it changes significantly with the normal stress (Cui, 2019; Jing et al. 1994). But because of the complexity of the jointing and uncertainty of the normal stress distribution, comprehensive stiffness data is still not available for joints in various rock types (Kulatilake et al. 2016). Thus, it is more common to adopt empirical formula for the estimation of the joint stiffness. From the back-calculation based on deformability information of intact rock and jointed rock mass, the following formula proposed by (HART 1993) is used for approximating the normal stiffness of joints k_n

$$k_n = \frac{E \times E_r}{s(E_r - E)} \tag{5}$$

where E is the elastic modulus of intact rock material; E_r is the elastic modulus of rock mass; s is the joint spacing. In

the study, E is taken as the dynamic elastic modulus of virgin rock in Table 3. E_r is assumed to be one-tenth of the elastic modulus of intact rock (Barton 1972). Thus, if the joint spacing is 0.5 m, k_n is calculated to be approximately as 10GPa/m by Eq. (5). The joint shear stiffness is assumed to be 0.5 of corresponding normal stiffness (Burdekin et al. 1979). In addition, for granite rock mass, the joint friction angle and cohesion are assumed to be 36° and 0.5 MPa, respectively (Horváth et al., 2012; Özvan et al., 2014).

Tunnel damage evaluating indicator

The blast-induced damage zones (BIDZ) were adopted as the evaluation indicators of tunnel damage in the study. BIDZ usually refers to the area where the strength or stiffness of rock mass is significantly attenuated under the blasting shock (Shen et al. 1997), and it may be characterized by cracks, sliding or even falling. The depth of the BIDZ has been widely used to evaluate the extent of damage to the surrounding rock (Sjoberg 1979; Sjoberg et al. 1997).

In jointed rock masses, the joint displacement has an important influence on the tunnel stability. According to the movement of joints, Shen et al. (1997) divided the rock damage zones near tunnel contour into failure zone, open zone and shear zone. The failure zone refers to the area where the rock blocks has been detached and falling into the tunnel while open zone is the rock zones where joints are displaced, and the shear zone where a certain shear displacement occurs. Among the three zones, the failure zone has a direct impact on tunnel stability, while the open zone and the shear zone are related to the groundwater seepage in the rock masses (Barton et al. 1985; Makurat et al. 1991). Since most open zones are close to the tunnel contour, even if the rock blocks in the zone do not fall off instantly after blasting, it will leave potential threats to the tunnel stability, such as the seepage causing pressure on the primary lining or further expansion of cracks activated under seismic load. Accordingly, the failure zone and the open zone are considered as the BIDZ, in which the open zones where joints displacement exceeds 0.01 m are regarded as BIDZ. As shown in Fig. 6, where the red zone is the failure zone and green zone is the open zone.

Parameter studies

In the section, some parameters are investigated, including joint inclination angle, joint spacing, joint strike angle, joint normal stiffness, tunnel depth and advance length, which appear to be significant factors affecting tunnel stability (Chakraborty et al. 1994a; Deng et al. 2014; Jia and Tang 2008; Shen and Barton 1997). The followings will provide a more detailed description of the value range for these factors.

Fig. 6 Diagram of blast-induced damage zone in this study

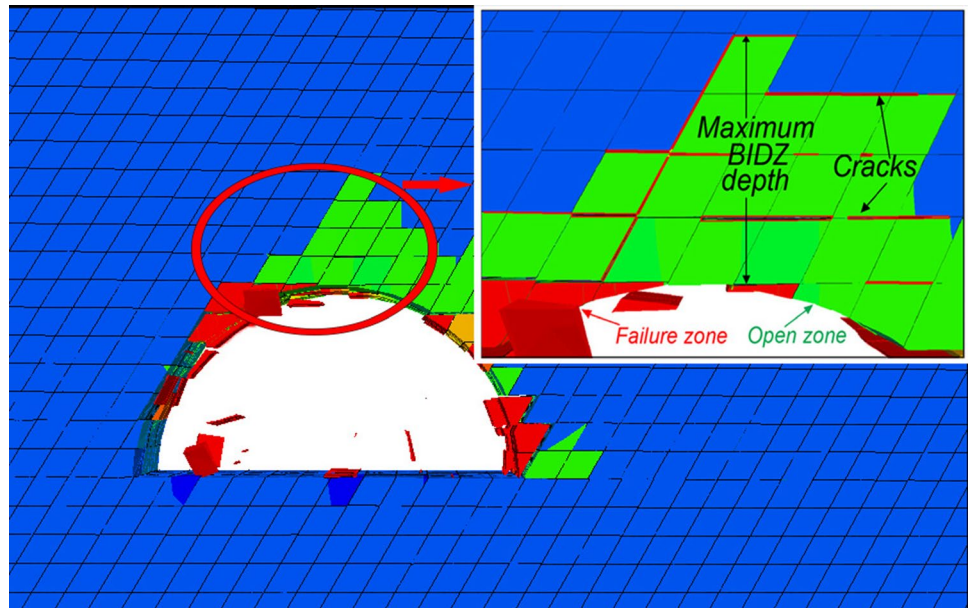
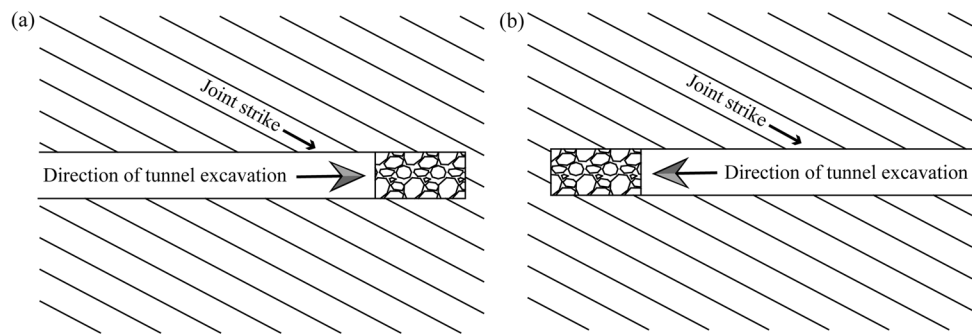


Fig. 7 The relationship between the direction of tunnel excavation and joint strike



As shown in Fig. 8, three intersected persistent joints are added to the model. In the study, the joint inclination angle is defined as the angle between the two sets of joints in the XY plane, and the joint strike angle is referred to the angle between joint strike and tunnel axis. To adequately consider the influence of the joint inclination, its range is assumed from 15° to 90° while fixing the level of one set of joints in XY plane.

For the joint strike, in general, when the direction of tunnel excavation is the same as the joint strike, it is usually referred to as driving with strike as shown in Fig. 7a, and the inverse is as driving against strike, as shown in Fig. 7b. The RMR rock mass classification system proposed by the South African Council of Scientific and Industrial Research (CSIR) indicates that tunneling with the joint strike is more beneficial than driving against joint strike (Bieniawski 1979). As shown in Table 4, effects of joint strike can be considered as favorable or very favorable when driving with strike. Therefore, to consider the adverse effect of joint strike angle on excavation damage, assuming that the tunnel excavation is driving against strike. The strike angles are set from 15° to

Table 4 Effect of Discontinuity Orientation and Strike in tunneling (Bieniawski, 1984)

Orientation of strike	Dip	
	20-45°	45-90°
Drive with strike	Favorable	Very Favorable
Drive against strike	Unfavorable	Fair
Parallel to tunnel axis	Fair	Very Unfavorable

75°. Noted that in the case of strike angle 0° and 90°, there will be an overlap of two sets of joints in YZ plane, so the strike angle 0° and 90° are not analyzed in the part.

For rock mass with natural joints, the joint spacing differs widely. The suggestion from the China railway sector that rock mass with single set of joints is classified according to the difference in joint spacing between 0 m and 1.0 m, as shown in Table 5. But if the joint spacing is set 0.1 m in the 3DEC model, it will consume enormous computational resources and even lead to breakdown. Hence, the joint spacing ranges are from 0.25 m to 1.0 m with an interval of

Table 5 Classification of rock mass based on joint spacing

Rock classification with a set of joints	Joint spacing S_j
Giant thickness	$1.0m \leq S_j$
General thickness	$0.5m \leq S_j \leq 1.0m$
Medium thickness	$0.1m \leq S_j \leq 0.5m$
Thin	$S_j \leq 0.1m$

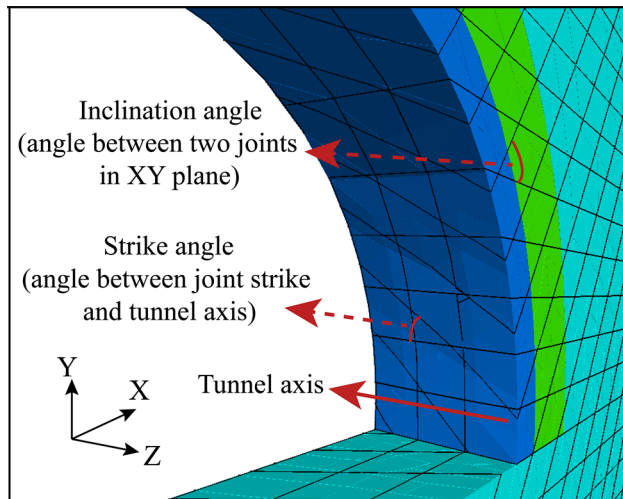


Fig. 8 Diagram of joint inclination angle and strike angle

0.25 m (Fig. 8). Besides, the normal stiffness also varies for joints with different normal stress, roughness or fillings (Bandis et al. 1981; Muralha et al. 2014). In the model, we assumed that the joint normal stiffness is 2.5GPa~40GPa to consider different strength joints.

At present, more than 50% of tunnels in China were buried in challenging geotectonic belts with depths of more than 100 m, and most were excavated using conventional drill and blast method (Zhou et al. 2021). Besides, the trial calculations revealed that there was very little blast-induced damage when the burial depth exceeded 600 m due to in situ stress, as shown in Fig. 13. Therefore, we assumed the tunnel burial depth range as 100 m-600 m with an interval of 100 m.

In the numerical model, the thickness of 3DEC model was changed to simulate different advance lengths. The commonly used advance length of tunnels constructed by D and B is approximately 2 m-5 m (Costamagna et al. 2018; Foderà et al. 2020; Zare and Bruland 2007). Additionally, it is notable that a blast round length-to-diameter ratio exceeding 2.0 was accomplished in the Canada Underground Research Laboratory (Kuzyk et al. 1995). However, due to the complexity of geologic conditions, the quality of boreholes is very hard to be guaranteed in the field application. Thus, we only added extra model thickness of 6 m and 7 m to denote larger round lengths.

In summary, the value range of the selected parameters is shown in Table 6. To analyze the effect of single factor, it is also necessary to choose a typical value for these parameters, i.e., when one variable is studied, a constant value for other parameters. For the joint inclination, after trial calculation, it was found that when the angle exceeded 60°, the tunnel damage increased significantly, so the inclination angle 60° was selected as the typical value. For joint strike angle, the typical value is assumed to be 0°, i.e., the joint strike is parallel to the tunnel axis. The constant value of joint spacing is assumed to be 0.5 m to consider the calculation efficiency. The corresponding joint normal stiffness is 10GPa from Eq. (5) as mentioned before. The typical values of tunnel buried depth and advance length are assumed to be 100 and 3 m respectively (Iverson et al. 2008; Zhao et al. 2013).

Besides, since wave attenuation in rock masses is mainly caused by joints in this model, the damping of original rock was neglected (King et al. 1986; Pyrak-Nolte et al. 1990).

Effect of joints on the damage of tunnel

Joint inclination angle

Figure 9 shows the BIDZ distribution after blasting loading at different joint inclination angles. It can be seen that when the joint angle is 15°, there is no visible damage zone around the contour. With the increase of the joint angle, the BIDZ gradually enlarges. When the joint angle is 30° to 60°, the failure zone is concentrated in the vault and shoulder positions. Furthermore, it can be clearly revealed that BIDZ range reaches the maximum at the joint angles of 75° and 90°, and destabilization disruption occurs in the vault rock masses.

Joint strike angle

The tunnel damage at different joint strike angles is shown in Fig. 10. It can be observed that the depth of tunnel damage zone is increased gradually as the strike angle approaches more vertical in relation to the tunnel axis. When the joints

Table 6 The range of values for different parameters

Parameter	Value
Joint inclination angle (°)	15,30,45,60,75,90
Joint strike angle (°)	15,30,45,60,75
Joint spacing (m)	0.25,0.5,0.75,1.0
Joint normal stiffness (GPa)	2.5,5,10,20,40
Tunnel depth (m)	100,200,300,400,500,600
Advance length (m)	2,3,4,5,6,7

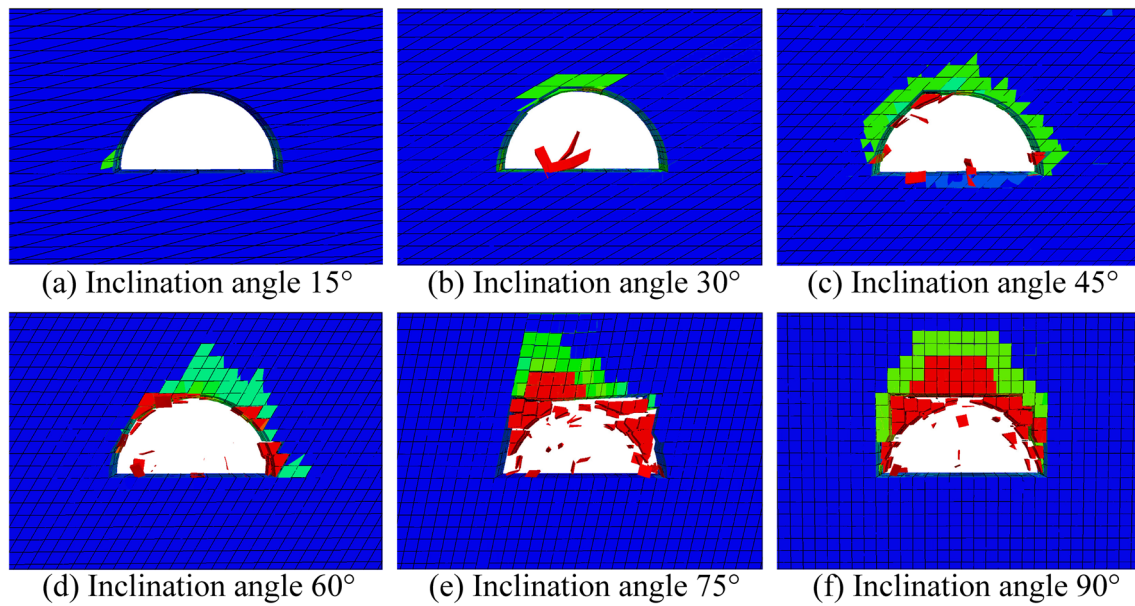


Fig. 9 Tunnel damage in terms of different joint inclination angles

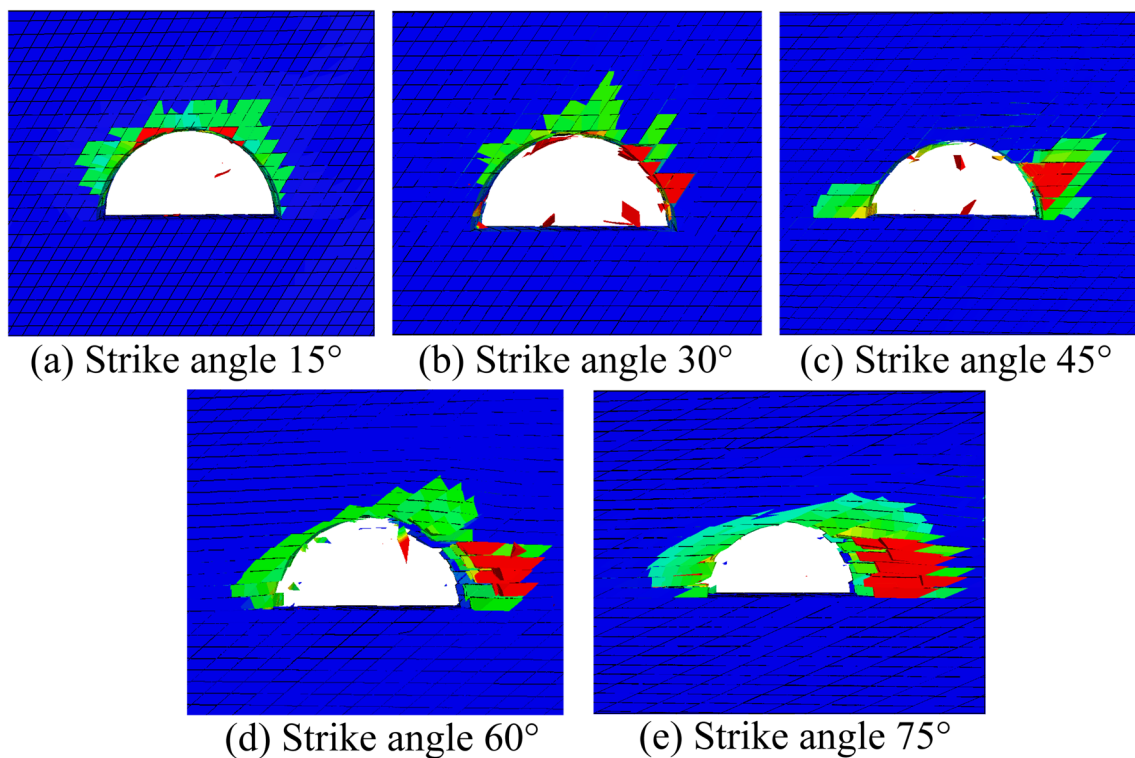


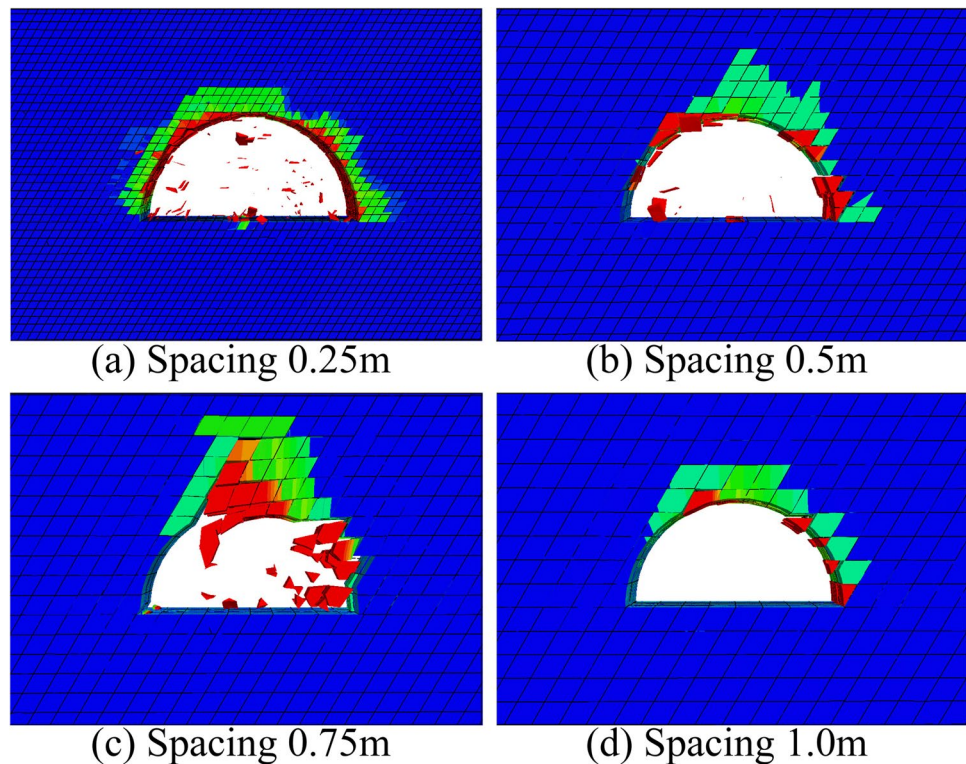
Fig. 10 Tunnel damage in terms of different joint strike angles

are close to horizontal (i.e., dip angle 15°), the failure zone is mainly in the tunnel vault. As the joint dip angle increases to $30^\circ \sim 75^\circ$, the failure zone is transferred to the right side the tunnel wall.

Joint spacing

Figure 11 presents damage condition with changing the joint spacing. It can be observed that the maximum depths of

Fig. 11 Tunnel damage in terms of different joint spacings



BIDZ at joint spacing of 0.25 m and 1 m are very similar without obvious failure zones. The damage depth at joint spacing of 0.5 m is at the middle value and there is a noticeable failure zones on the left shoulder. The tunnel damage is most severe when the joint spacing is 0.75 m. It is worth noting that the damage extent is not increased or decreased with increasing joint spacing.

Joint normal stiffness

Figure 12 show the tunnel damage for different joint stiffness. It can be found that the range of the failure zones gradually decreases when the joint stiffness varies from 2.5 GPa to 10 GPa. The tunnel is relatively stable when the joint stiffness is 20GPa~40GPa because there are almost no obvious failure zones in the surrounding rock.

Effect of initial stress distribution and advance length

Tunnel depth

Figure 13 displays the distribution of tunnel damage under blasting loading in the varied tunnel depths. It can be seen that the damage area gradually decreases with the rising of tunnel depth, but the magnitude of the change is not obvious. When the buried depth increases to 600 m, only a very few

rock blocks fall from the left shoulder and there are almost no failure zones in the surrounding rock.

Advance length

Figure 14 shows the surrounding rock damage at different advance lengths. It can be clearly seen that when the advance length is 2 m, there is no visible failure zones around the tunnel surface. With the increase in the advance length, the tunnel damage range extends considerably. When the advance length reaches 7 m, the vault rock mass has the tendency to fall down.

Sensitivity analysis

Figure 15 shows the arithmetic mean of maximum damage depth and its standard deviation for different calculated cases above. The standard deviation reflects the dispersion of the individual data in every dataset, and it is used to show the impact extent of a change in one of the above conditions on the tunnel damage, where the smaller the standard deviation means that the impact of the factor on tunnel damage is relatively insignificant. It can be seen that the arithmetic mean and standard deviation of maximum damage depth in different advance length are greater than other factors, which reveals that the tunnel damage by increasing the advance length is more severe compared to the geometrical and mechanical properties of joints and tunnel depth.

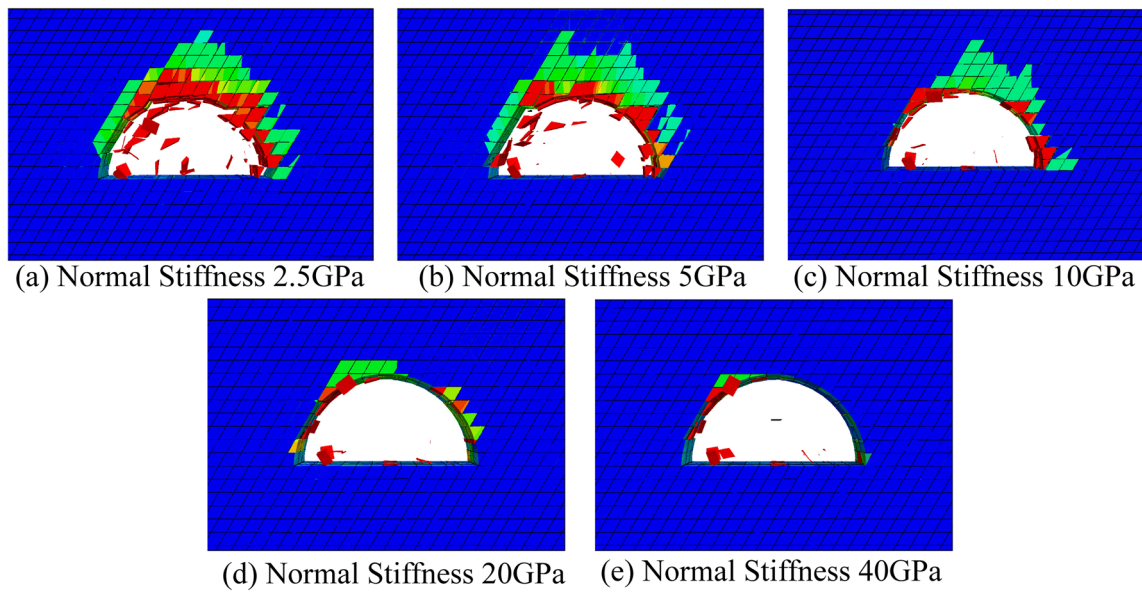


Fig. 12 Tunnel damage in terms of different joint normal stiffness

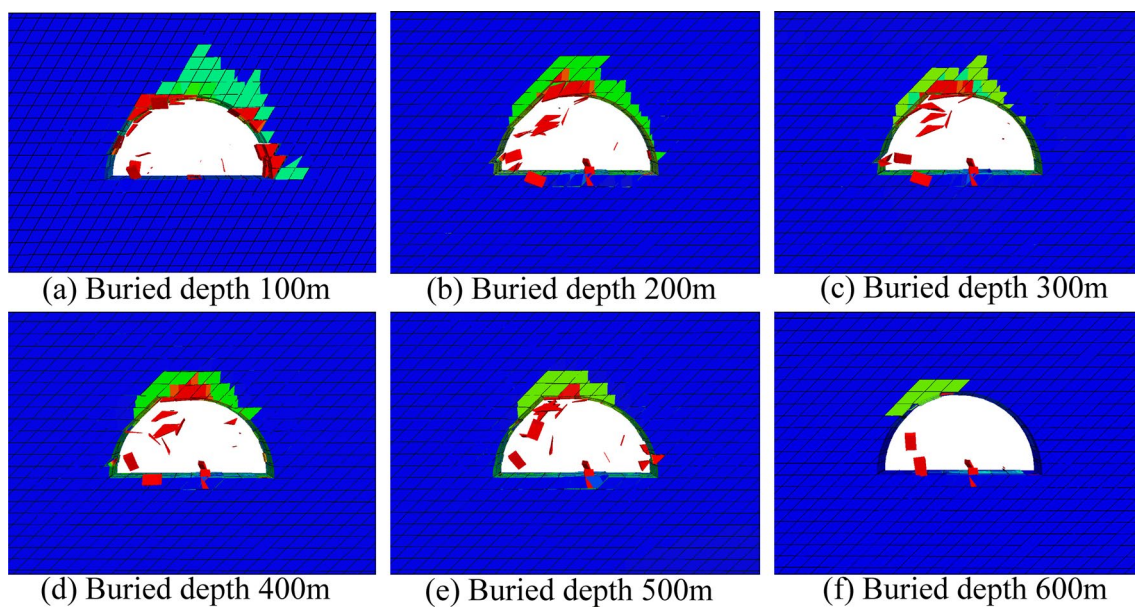


Fig. 13 Tunnel damage in terms of different buried depths

Figure 16 shows the peak particle velocity (PPV) at the tunnel left shoulder in different advance lengths. A remarkable increase of PPV can be found when the advance length is changed from 2 to 3 m, which is also consistent with Fig. 14 where the failure zone begins to develop when the advance length is above 2 m. Besides, damage depth and standard deviation as increasing tunnel buried depths are

the smallest among these factors, which means that the buried depth could have more minor effect on tunnel damage. Besides, in the joint geometric factors including inclination, strike and spacing, the damage depth under different strike angles is higher, but its standard deviation is relatively small. It can also be found from Fig. 10 that the tunnels with varied joint strike angles all contain visible damage zones.

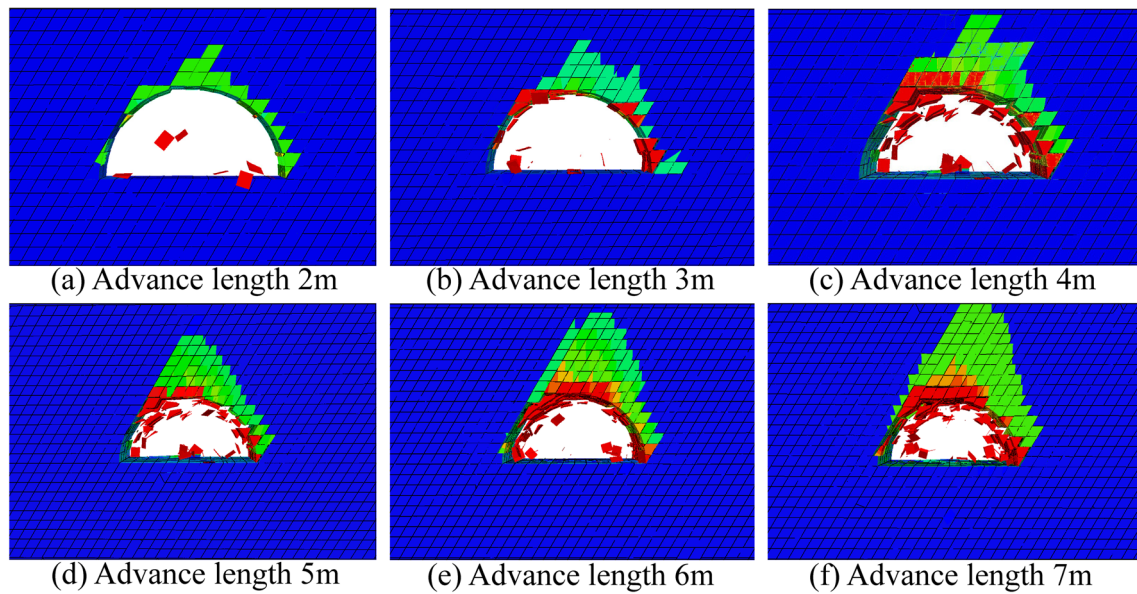


Fig. 14 Tunnel damage in terms of different advance lengths

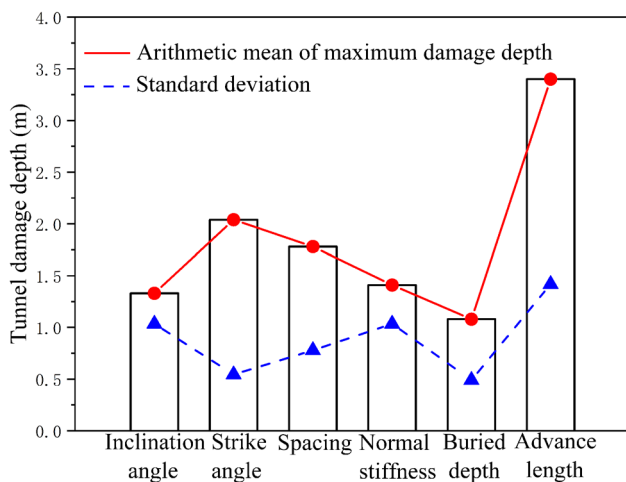


Fig. 15 Arithmetic mean of maximum damage depth and standard deviation in different cases

Discussion

For the estimation of tunnel damage zones excavated by drill and blast method, researchers have proposed some empirical formulas from different aspects, many of which are based on a single factor such as the charge density, maximum charge per delay or peak particle velocity (Dowding 1984; Kwon et al. 2006; Pusch and Stanfors 1992; Zhou 2011).

Comparatively, the damage extent estimation formula developed by Verma et al. (2018) integrated the explosive

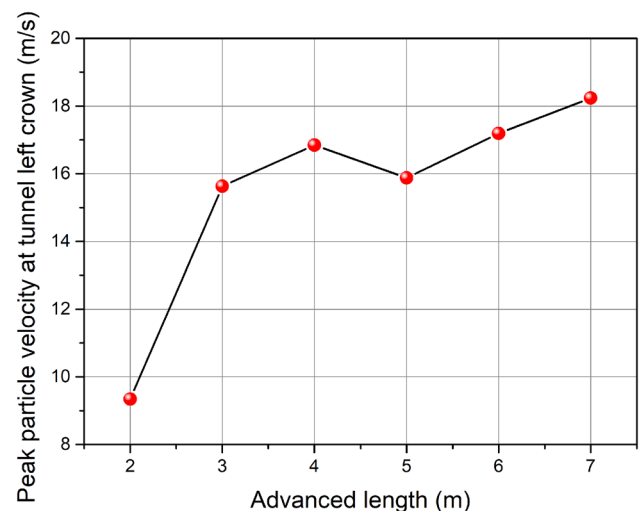


Fig. 16 Peak particle velocities at tunnel left roof in terms of different advanced length

charge, borehole depth, cross-sectional area and rock mass quality. Thus, the formula is used to contrast with the results of this study:

$$D_d = 0.96 \left[\frac{q_p^{0.15} \sqrt{W + q}}{Q^{0.33}} \left(\frac{C_f}{A_f} \right)^{0.15} \right] - 1.28 \tag{6}$$

$$C_f = \frac{d}{a} \tag{7}$$

Table 7 Calculation parameters of the empirical formula

Parameters	Value
Specific charge q (kg/m ³)	1.2
Maximum charge W (kg)	70
Perimeter charge factor q_p (kg/m ³)	3
Advance length l (m)	2,3,4,5,6,7

Table 8 Rock mass scores for different joint configurations

Joint configuration	Range	RMR system	Q system
Inclination angle	15° ~ 90°	62 ~ 50	100 ~ 4.64
Spacing	0.25 m ~ 1 m	50 ~ 55	4.64 ~ 16.68
Strike angle	15° ~ 75°	52 ~ 57	7.74 ~ 27.83

$$A_f = \frac{l}{d} \quad (8)$$

where D_d is the damage depth, q_p is the perimeter charge factor, W is the maximum charge per day, q is the specific charge, Q is the rock mass quality index (Barton' Q-system), d is the hole depth, l is the advance length, a is the tunnel cross-sectional area.

In comparison with the Q system, the RMR system considers the effects of joint inclination, strike and spacing on the tunnel structure. Therefore, we use the Eq. (9) to convert the rock mass scores from RMR system to Q system (Bieniawski 1989).

$$Q = 10^{\frac{\text{RMR} - 44}{10}} \quad (9)$$

The tunnel damage depth for different joint inclination angles, strike angles, spacings and advance lengths were compared with the Eq. (6). The detailed parameters used for the calculation are shown in Table 7, which refer to the commonly adopted drill and blast schemes in the tunnel excavation (Wang 2015). The tunnel cross-sectional area a in the model is 19.24m². The value of the confinement factor C_f varies with the advance length l . The advancement factor A_f is assumed to be 1 (i.e., the hole depth d equal to the advance length l). The scoring values of RMR system for different joint inclination angles, spacings and strike angles are shown in Table 8. These values are acquired according to the rock and joint characteristics of the model, and referenced to the RMR classification system (Bieniawski 1989), and then converted to Q system by Eq. (9).

From Fig. 17a, it can be seen that the damage depth at different joint inclination angles is consistent with the empirical method of Verma et al. Moreover, when the

inclination angle is less than 45°, the damage depth is in the range of 1 m, and if the inclination is greater than 60°, the damage depth may be deeper than 2 m. It is also comparable to the RMR system (Bieniawski 1993), where inclination angles of 20° ~ 45° and 45° ~ 90° are considered as fair and unfavorable, respectively. It should also be observed that when the joints parallel to the tunnel axis, the failure zones are mainly found in the upper part of the tunnel as shown in Fig. 9, indicating that the rock reinforcement in proximity to the tunnel top should be given enough attention in the condition.

However, the damage depth between the model and estimated value shows significantly opposite tendency as the strike angle increasing, as shown in Fig. 17b. This is because the RMR system regards that a larger joint strike is relatively beneficial to tunnel stability. But under the internal blasting effect, when the joints are more perpendicular to the tunnel axis, the blast wave is less affected by the joints and so is prone to cause more damage in the surrounding rock (Chakraborty et al. 1994a, 1994b). Thus, as the joint strike angle increases, the number of blastholes or explosive density should be decreased correspondingly. It is noted that this study concentrates more on the tunnel damage under the internal blasting. If blasting charges are well controlled or if excavation is conducted by mechanical methods (e.g., Tunnel Boring Machine), driving against joint dip is still detrimental to the tunnel structure (Delisio et al. 2013; Einstein et al. 2006).

In the computational model, there is a significant dispersion for tunnel damage depth at joint spacing from 0.25 m to 1.0 m, as shown in Fig. 17c. In general, a smaller spacing of joints implies more numbers of joints and thus is detrimental to the tunnel stability (Barton 2013; Wang et al. 2013). But on another side, more joints will absorb more blast wave energies and reduce the blast-induced surrounding rock damage (Lanari and Fakhimi 2015). Therefore, for tunnels excavated by drill and blast, the increase in the joint spacing does not induce in increasing or decreasing tendency of tunnel damage zones. This phenomenon was also found for the jointed tunnel response subject to external blast shock (Deng et al. 2014).

The increased joint stiffness makes the tunnel more stable, as shown in Fig. 12. This is mainly because the greater stiffness limits the opening of the joints (Bandis et al. 1983). Furthermore, the increasing buried depth (i.e., in-situ stress) also restricts the crack growth (Tao et al. 2020; Xie et al. 2016), and the model obtained similar results, as shown in Fig. 13. However, it should be noted that in the excavation of deeper tunnel, the BIDZ may be further extended and the surrounding rock may be damaged persistently due to stress redistribution, underground pressurized water or creep of rock masses (Hedayat and

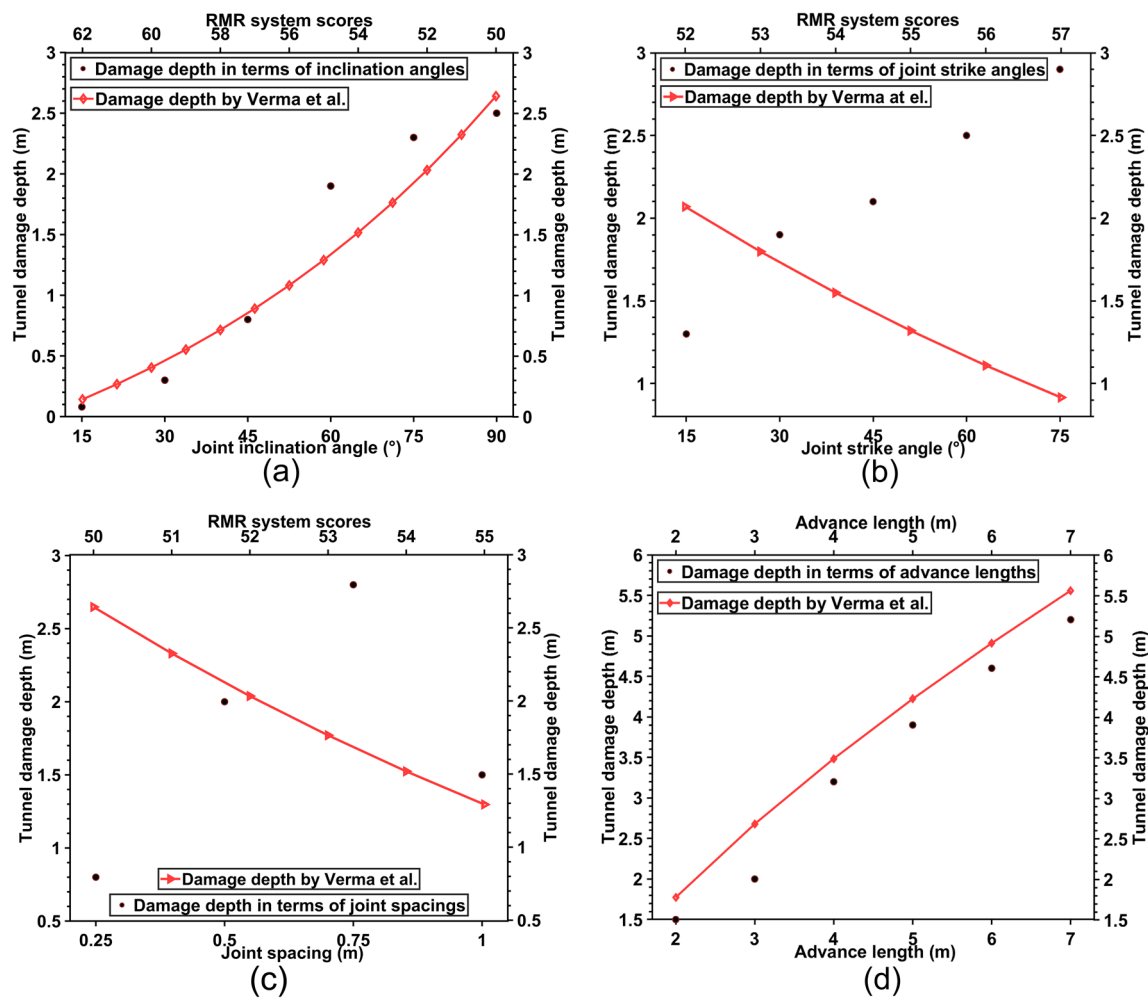


Fig. 17 Comparison of the results of this study with an empirical formula: **a** Joint inclination angle; **b** Joint strike angle; **c** Joint spacing; **d** Advance length

Weems 2019; Wang et al. 2016). Therefore, the range of damage zones may need to further explored for some larger buried tunnels.

The tunnel damage is significantly more severe with the increase in the advance length, and this is also consistent with the empirical estimated results, as shown in Fig. 14 and Fig. 17d. It indicates that if the drill and blast method is used to excavate jointed tunnels, the advance length should be cautiously controlled.

Conclusions

This study develops a numerical approach to evaluate the damage extent for a jointed tunnel excavation subjected to internal blasting shock using DEM-based code 3DEC. Some parameters that may affect tunnel stability were investigated and a sensitivity analysis for these factors was performed.

Lastly, several comparisons were conducted with existing empirical evaluation formulas for tunnel damage. The main conclusion are presented as follows:

- (1) The numerical model considers both excavation and internal blast effects by converting the blasting load into a stress-time history on the tunnel contour. The evaluation of tunnel damage for various factors is performed through failure and open zones.
- (2) Under the internal blasting load, the tunnel damage is more critical as the joint inclination and strike angle increases. The vault rocks of the tunnel are liable to fall when joints are parallel to tunnel axis, and as the strike angle increases, the failure zones are mainly in the sidewall, so the rock mass at these positions should be reinforced carefully in above conditions.
- (3) The magnitude of tunnel damage could not be evaluated simply by increasing or decreasing the joint spacing in the dynamic loading condition. An increase in

buried depth (i.e., higher in-situ stress) or joint stiffness is beneficial in reducing tunnel blast damage. But the tunnel depth in this study is limited within 600 m, and the damage zones at deeper levels should be further investigated.

- (4) The result of the sensitivity analysis shows that the increase in the advance length will have a more significant adverse effect on tunnel damage than the joint parameters and buried depth. Thus, for jointed tunnels, increasing advance length per round should be considered cautiously.
- (5) In the research, tunnel damage was only evaluated for a single factor variation. For tunnel excavation in the more complex geological situation, some unfavorable factors probably occur in combination, so it is necessary to evaluate the combined effect using real case in the future.

Author contribution All authors contributed to the study conception and design. Material preparation, data collection and analysis were performed by SC and ZZ. The first draft of the manuscript was written by SC and all authors commented on previous versions of the manuscript. All authors read and approved the final manuscript.

Funding Partial financial support was received from the National Natural Science Foundation of China (51978424).

Data availability Data will be made available on request.

Declarations

Conflict of interest The authors have no relevant financial or non-financial interests to disclose.

References

- Azarafza M, Asghari-Kalajahi E, Akgün H (2017) Numerical modeling of discontinuous rock slopes utilizing the 3DDGM (three-dimensional discontinuity geometrical modeling) method. *Bull Eng Geol Env* 76:989–1007
- Azarafza M, Akgün H, Asghari-Kalajahi E (2018) Stochastic geometry model of rock mass fracture network in tunnels. *Q J Eng Geol-Hydrogeol* 51:379–386
- Bandis S, Lumsden A, Barton N (1981) Experimental studies of scale effects on the shear behaviour of rock joints. In: *International journal of rock mechanics and mining sciences and geomechanics abstracts*, Elsevier, England, pp 1–21
- Bandis S, Lumsden A, Barton N (1983) Fundamentals of rock joint deformation. In: *International journal of rock mechanics and mining sciences and geomechanics abstracts*. Elsevier, England, pp 249–268
- Barton N (1972) A model study of rock-joint deformation. *International journal of rock mechanics and mining sciences and geomechanics abstracts*. Elsevier, England, pp 579–582
- Barton N (2013) Shear strength criteria for rock, rock joints, rockfill and rock masses: problems and some solutions. *J Rock Mech Geotech Eng* 5:249–261. <https://doi.org/10.1016/j.jrmge.2013.05.008>
- Barton N, Bandis S, Bakhtar K (1985) Strength, deformation and conductivity coupling of rock joints. In: *International journal of rock mechanics and mining sciences and geomechanics abstracts*. Elsevier, England, pp 121–140
- Bieniawski ZT (1989) *Engineering rock mass classifications: a complete manual for engineers and geologists in mining, civil, and petroleum engineering*. John Wiley & Sons, United States
- Bieniawski ZT (1993) 22 - Classification of Rock Masses for Engineering: The RMR System and Future Trends. In: Hudson JA (ed) *Rock Testing and Site Characterization*. Pergamon, Oxford, pp 553–573
- Bieniawski Z (1979) The geomechanics classification in rock engineering applications. 4th ISRM Congress. OnePetro
- Bieniawski ZT (1984) Rock mechanics design in mining and tunneling
- Burdekin M, Back N, Cowley A (1979) Analysis of the local deformations in machine joints. *J Mech Eng Sci* 21:25–32
- Cai Y, Zhu H, Zhuang X (2013) A continuous/discontinuous deformation analysis (CDDA) method based on deformable blocks for fracture modeling. *Front Struct Civ Eng* 7:369–378
- Chakraborty A, Jethwa J, Paithankar A (1994a) Effects of joint orientation and rock mass quality on tunnel blasting. *Eng Geol* 37:247–262
- Chakraborty AK, Jethwa JL, Paithankar AG (1994b) Assessing the effects of joint orientation and rock mass quality on fragmentation and overbreak in tunnel blasting. *Tunn Undergr Space Technol* 9:471–482. [https://doi.org/10.1016/0886-7798\(94\)90106-6](https://doi.org/10.1016/0886-7798(94)90106-6)
- Costamagna E, Oggeri C, Segarra P, Castedo R, Navarro J (2018) Assessment of contour profile quality in D&B tunnelling. *Tunn Undergr Space Technol* 75:67–80. <https://doi.org/10.1016/j.tust.2018.02.007>
- Cui Y (2019) Effect of joint type on the shear behavior of synthetic rock. *Bull Eng Geol Env* 78:3395–3412
- Delisio A, Zhao J, Einstein HH (2013) Analysis and prediction of TBM performance in blocky rock conditions at the Löttschberg Base Tunnel. *Tunn Undergr Space Technol* 33:131–142
- Deng X, Zhu J, Chen S, Zhao Z, Zhou Y, Zhao J (2014) Numerical study on tunnel damage subject to blast-induced shock wave in jointed rock masses. *Tunn Undergr Space Technol* 43:88–100
- Dey K, Murthy V (2012) Prediction of blast-induced overbreak from uncontrolled burn-cut blasting in tunnels driven through medium rock class. *Tunn Undergr Space Technol* 28:49–56
- Dowding CH (1984) Estimating earthquake damage from explosion testing of full-scale tunnels. *Adv Tunn Technol Subsurf Use* 4:113–117
- Einstein H, Bobet A, Karam K (2006) Report on TBM–Penetration, TBM Wear, Face Instabilities. Unpublished Report, BLS AlpTransit Nachforderungen MaTrans
- Foderà G, Voza A, Barovero G, Tinti F, Boldini D (2020) Factors influencing overbreak volumes in drill-and-blast tunnel excavation. a statistical analysis applied to the case study of the Brenner Base Tunnel–BBT. *Tunn Undergr Space Technol* 105:103475
- Han X, Chen J, Wang Q, Li Y, Zhang W, Yu T (2016) A 3D fracture network model for the undisturbed rock mass at the Songta dam site based on small samples. *Rock Mech Rock Eng* 49:611–619
- HART RD (1993) An introduction to distinct element modeling for rock engineering. In: *Analysis and Design Methods*, Elsevier, England, pp 245–261
- Hedayat A, Weems J (2019) The elasto-plastic response of deep tunnels with damaged zone and gravity effects. *Rock Mech Rock Eng* 52:5123–5135. <https://doi.org/10.1007/s00603-019-01834-4>
- Holmberg R (1979) *Design of tunnel perimeter blasthole patterns to prevent rock damage*. Maney publishing, England
- Horváth Z, Megyeri T, Váró Á, Görög P (2012) Discrete element modelling of the Mórág granite formation in Southern Hungary. 1st

- Eastern European Tunneling Conference Magyar Alagútépítő Egyesület, Budapest, Paper
- Iverson S, Kerkering C, Hustrulid W (2008) Application of the NIOSH-modified Holmberg-Persson approach to perimeter blast design. *Proceedings Of The 34th Conference On Explosives And Blasting Technique*. pp 1–33
- Jia P, Tang CA (2008) Numerical study on failure mechanism of tunnel in jointed rock mass. *Tunn Undergr Space Technol* 23:500–507. <https://doi.org/10.1016/j.tust.2007.09.001>
- Jing L, Nordlund E, Stephansson O (1994) A 3-D constitutive model for rock joints with anisotropic friction and stress dependency in shear stiffness. In: *International journal of rock mechanics and mining sciences and geomechanics abstracts*, Elsevier, England, pp 173–178
- King MS, Myer LR, Rezowalli JJ (1986) Experimental studies of elastic-wave propagation in a columnar-jointed rock mass. *Geophys Prospect* 34(8):1185–1199
- Koopialipoor M, Jahed Armaghani D, Haghghi M, Ghaleini EN (2019) A neuro-genetic predictive model to approximate over-break induced by drilling and blasting operation in tunnels. *Bull Eng Geol Env* 78:981–990
- Kulatilake PH, Shreedharan S, Sherizadeh T, Shu B, Xing Y, He P (2016) Laboratory estimation of rock joint stiffness and frictional parameters. *Geotech Geol Eng* 34:1723–1735
- Kuzyk G, Onagi D, Keith S, Karklin G (1995) The development of long blast rounds at AECL's underground research Laboratory. *Miner Resour Eng* 4:225–235
- Kwon S, Cho W, Han P (2006) Concept development of an underground research tunnel for validating the Korean reference HLW disposal system. *Tunn Undergr Space Technol* 21:203–217
- Lanari M, Fakhimi A (2015) Numerical study of contributions of shock wave and gas penetration toward induced rock damage during blasting. *Comput Part Mech* 2:197–208
- Li X, Cao W, Zhou Z, Zou Y (2014) Influence of stress path on excavation unloading response. *Tunn Undergr Space Technol* 42:237–246
- Lu W, Yang J, Chen M, Zhou C (2011) An equivalent method for blasting vibration simulation. *Simul Model Pract Theory* 19:2050–2062
- Lu W, Yang J, Yan P, Chen M, Zhou C, Luo Y, Jin L (2012) Dynamic response of rock mass induced by the transient release of in-situ stress. *Int J Rock Mech Min Sci* 53:129–141. <https://doi.org/10.1016/j.ijrmms.2012.05.001>
- Makurat A, Barton N, Rad NS, Bandis S. (1991) Joint conductivity variation due to normal and shear deformation. 182:1-6
- Malmgren L, Nordlund E (2006) Behaviour of shotcrete supported rock wedges subjected to blast-induced vibrations. *Int J Rock Mech Min Sci* 43:593–615
- Martino J, Chandler N (2004) Excavation-induced damage studies at the underground research laboratory. *Int J Rock Mech Min Sci* 41:1413–1426
- Monsalve JJ, Baggett J, Bishop R, Ripepi N (2019) Application of laser scanning for rock mass characterization and discrete fracture network generation in an underground limestone mine. *Int J Min Sci Technol* 29:131–137
- Muralha J, Grasselli G, Tatone B, Blümel M, Chryssanthakis P, Yujing J (2014) ISRM suggested method for laboratory determination of the shear strength of rock joints: revised version. *Rock Mech Rock Eng* 47:291–302
- Ning Y-J, An X-M, Lü Q, Ma G-W (2012) Modeling rock failure using the numerical manifold method followed by the discontinuous deformation analysis. *Acta Mech Sin* 28:760–773
- Özvan A, Diñçer İ, Acar A, Özvan B (2014) The effects of discontinuity surface roughness on the shear strength of weathered granite joints. *Bull Eng Geol Env* 73:801–813. <https://doi.org/10.1007/s10064-013-0560-x>
- Pusch R, Stanfors R (1992) The zone of disturbance around blasted tunnels at depth. In: *International journal of rock mechanics and mining sciences and geomechanics abstracts*. Elsevier, England, pp 447–456
- Pyrak-Nolte LJ, Myer LR, Cook NG (1990) Anisotropy in seismic velocities and amplitudes from multiple parallel fractures. *J Geophys Res* 95:11345–58
- Read R (2004) 20 years of excavation response studies at AECL's Underground Research Laboratory. *Int J Rock Mech Min Sci* 41:1251–1275
- Saiang D (2010) Stability analysis of the blast-induced damage zone by continuum and coupled continuum–discontinuum methods. *Eng Geol* 116:1–11
- Shen B, Barton N (1997) The disturbed zone around tunnels in jointed rock masses. *Int J Rock Mech Min Sci* 34:117–126
- Shen B, Barton N (1997) The disturbed zone around tunnels in jointed rock masses. *Int J Rock Mech Min Sci* 34:117–126
- Sjoberg C, Larsson B, Lindstrom M, Palmqvist KJAp (1997) A blasting method for controlled crack extension and safety underground.
- Sjoberg C (1979) Cracking zones around slender borehole charges. *Proceedings of annual discussion meeting BK-79 Swedish rock construction committee*, Stockholm. pp 53–98
- Tao J, Yang X-G, Li H-T, Zhou J-W, Fan G, Lu G-D (2020) Effects of in-situ stresses on dynamic rock responses under blast loading. *Mech Mater* 145:103374. <https://doi.org/10.1016/j.mechmat.2020.103374>
- Trisugiwo M, Zabidi H, Ahmad F (2016) Joint Analysis to Evaluate Geological Over-break in Excavation of Surge Chamber Cavern. *Procedia Chem* 19:751–756. <https://doi.org/10.1016/j.proche.2016.03.080>
- Varma M, Maji V, Boominathan A (2019) Numerical modeling of a tunnel in jointed rocks subjected to seismic loading. *Undergr Space* 4:133–146
- Verma H, Samadhiya NK, Singh M, Goel R, Singh P (2018) Blast induced rock mass damage around tunnels. *Tunn Undergr Space Technol* 71:149–158
- Wang R (2015) Blasting vibration control techniques and influence assessment on qingdao metro line. *Blasting* 32:139–145 ((In Chinese))
- Wang S, Ni P, Guo M (2013) Spatial characterization of joint planes and stability analysis of tunnel blocks. *Tunn Undergr Space Technol* 38:357–367. <https://doi.org/10.1016/j.tust.2013.07.017>
- Wang T, Hu W, Wu H, Zhou W, Su K, Cheng L (2016) Seepage analysis of a diversion tunnel with high pressure in different periods: a case study. *Eur J Environ Civ Eng* 22:386–404. <https://doi.org/10.1080/19648189.2016.1197159>
- Wang L, Chen W, Tan X, Tan X, Yang J, Yang D, Zhang X (2020) Numerical investigation on the stability of deforming fractured rocks using discrete fracture networks: a case study of underground excavation. *Bull Eng Geol Env* 79:133–151
- Xiao LC, Quan JJ (2002) Numerical simulation of slope stability, with 3DEC, and verification in field, by the GPR. *ISRM International Symposium-EUROCK 2002*. OnePetro
- Xie L, Lu W, Zhang Q, Jiang Q, Wang G, Zhao J (2016) Damage evolution mechanisms of rock in deep tunnels induced by cut blasting. *Tunn Undergr Space Technol* 58:257–270
- Yan P, Zhou W, Lu W, Chen M, Zhou C (2016) Simulation of bench blasting considering fragmentation size distribution. *Int J Impact Eng* 90:132–145. <https://doi.org/10.1016/j.ijimpeng.2015.11.015>
- Yu S (2018) Limit analysis of a shallow subway tunnel with staged construction. *Geomech Eng* 15:1039–1046
- Zare S, Bruland A (2007) Progress of drill and blast tunnelling efficiency with relation to excavation time and costs. *Proceedings of the 33rd ITAAITES World Tunnel Congress*, Prague, Czech Republic. pp 805–809

- Zhang W, Xu B, Mei J, Yue G, Shi W (2020) A numerical study on mechanical behavior of jointed rock masses after tunnel excavation. *Arab J Geosci*. <https://doi.org/10.1007/s12517-020-05358-y>
- Zhang K, Xue Y, Xu Z, Su M, Qiu D, Li Z (2021) Numerical study of water inflow into tunnels in stratified rock masses with a dual permeability model. *Environ Earth Sci* 80:1–12
- Zhao Z, Zhang Y, Bao H (2011) Tunnel blasting simulations by the discontinuous deformation analysis. *Int J Comput Methods* 8:277–292
- Zhao Z, Jia H, Peng B, Dong Y (2013) Tunnel surrounding rock deformation characteristics and control in deep coal mining. *Geomaterials* 03(1):24–27
- Zhou Y (2011) Explosion loading and tunnel. *Advances in rock dynamics and applications*. CRC Press, London, p 457
- Publisher's Note** Springer Nature remains neutral with regard to jurisdictional claims in published maps and institutional affiliations.
- Springer Nature or its licensor (e.g. a society or other partner) holds exclusive rights to this article under a publishing agreement with the author(s) or other rightsholder(s); author self-archiving of the accepted manuscript version of this article is solely governed by the terms of such publishing agreement and applicable law.